Protein degradation corrects for imbalanced subunit stoichiometry in OST complex assembly

Susanne Mueller[a], Asa Wahlander[b], Nathalie Selevsek[b], Claudia Otto[c], Elsy Mankah Ngwa[a], Kristina Poljak[a], Alexander D. Frey[d], Markus Aebi[a], and Robert Gauss[a]

[a]Institute of Microbiology, Department of Biology, Swiss Federal Institute of Technology, ETH Zurich, CH-8093 Zurich, Switzerland; [b]Functional Genomics Center Zurich, UZH/ETH Zurich, CH-8057 Zurich, Switzerland; [c]Department of Health Sciences and Technology, Institute of Food, Nutrition and Health, ETH Zürich, CH-8092 Zurich, Switzerland; [d]Department of Biotechnology and Chemical Technology, Aalto University, FI-00076 Aalto, Finland

ABSTRACT **Protein degradation is essential for cellular homeostasis. We developed a sensitive approach to examining protein degradation rates in *Saccharomyces cerevisiae* by coupling a SILAC approach to selected reaction monitoring (SRM) mass spectrometry. Combined with genetic tools, this analysis made it possible to study the assembly of the oligosaccharyl transferase complex. The ER-associated degradation machinery compensated for disturbed homeostasis of complex components by degradation of subunits in excess. On a larger scale, protein degradation in the ER was found to be a minor factor in the regulation of protein homeostasis in exponentially growing cells, but ERAD became relevant when the gene dosage was affected, as demonstrated in heterozygous diploid cells. Hence the alleviation of fitness defects due to abnormal gene copy numbers might be an important function of protein degradation.**

Monitoring Editor
Reid Gilmore
University of Massachusetts

Received: Mar 23, 2015
Revised: May 11, 2015
Accepted: May 11, 2015

INTRODUCTION

Protein turnover is a process driven by loss of old and synthesis of new proteins. Replacement of proteins can be important for cellular processes such as the regulation of cell division (Lecker *et al.*, 2006). Furthermore, the interplay between transcription, translation, and protein degradation regulates protein abundance (Gygi *et al.*, 1999; Vogel and Marcotte, 2012). Balanced protein abundances are particularly important for formation of multiprotein complexes, and degradation might be a means to adjust protein levels according to subunit ratios. One cause of unbalanced protein expression is aneuploidy, by which one or numerous genes are missing or supernumerary. This condition results in proteotoxic stress; it is the main cause for mental retardation and a key characteristic of cancer cells (Weaver and Cleveland, 2006; Oromendia *et al.*, 2012; Oromendia and Amon, 2014; Duijf and Benezra, 2013).

Protein complexes fulfill many cellular functions; for example, the SEC translocon transports proteins into the endoplasmic reticulum (ER), the proteasome degrades cellular proteins, and the anaphase-promoting complex/cyclosome (APC/C) governs progression through the cell cycle. Another complex, the oligosaccharyl transferase (OST), is the central enzyme of asparagine-linked (N-) glycosylation and attaches glycans to N-X-S/T sequons on proteins in the ER lumen (Breitling and Aebi, 2013). In the yeast *Saccharomyces cerevisiae*, OST consists of eight proteins, including the two mutually exclusive thioreductases Ost3p and Ost6p. There is only limited information on OST assembly or degradation, but previous biochemical and genetic data suggested that assembly involves stable subcomplexes (Schwarz *et al.*, 2005; Kelleher and Gilmore, 2006). Analysis of other protein complexes showed that subunits stabilize each other during assembly and that proteins are incorporated into the complex in a defined sequence (Johnson *et al.*, 1998; Asher *et al.*, 2006; Daley, 2008).

ER-associated degradation (ERAD) accounts for the main part of protein degradation from the ER (Thibault and Ng, 2012). This pathway recognizes misfolded proteins at the ER and redirects them into the cytosol for proteasomal degradation (Ruggiano *et al.*, 2014). In yeast, the key components are two E3 ubiquitin ligase complexes, the HRD1 and DOA10 complexes, which recognize and ubiquitylate misfolded proteins. ERAD has mainly been studied by analyzing

This article was published online ahead of print in MBoC in Press (http://www.molbiolcell.org/cgi/doi/10.1091/mbc.E15-03-0168) on May 20, 2015.

Address correspondence to: Robert Gauss (robert.gauss@micro.biol.ethz.ch), Markus Aebi (markus.aebi@micro.biol.ethz.ch).

Abbreviations used: APC/C, anaphase-promoting complex/cyclosome; CPY, carboxy peptidase Y; ER, endoplasmic reticulum; ERAD, ER-associated degradation; MS, mass spectrometry; OST, oligosaccharyl transferase; PMT, protein O-mannosyl transferase; PrA, proteinase A; QTRAP, quadrupole ion trap; SEC, secretory; SRM, selected reaction monitoring; SILAC, stable isotope labeling by amino acids in cell culture.

mutated proteins that are rapidly degraded, such as PrA* and CPY* (Finger *et al.*, 1993; Xie *et al.*, 2009). In general, such studies use a pulse-chase setup to distinguish old from newly synthesized protein, which is coupled to SDS–PAGE–based methods for detection. Large-scale studies with this setup are impractical since only one protein is monitored per experiment. To increase the capacity of protein degradation studies in yeast, we coupled a pulse-chase approach based on stable isotope labeling by amino acids in cell culture (SILAC) to shotgun mass spectrometry (MS; Pratt *et al.*, 2002). This approach made it possible to determine degradation rates for hundreds of proteins in a single experiment. However, despite the progress in MS technologies and increasing sensitivity of mass spectrometers, consistent detection of low-abundance proteins remained difficult. Adapting this large-scale method for the analysis of low-abundance proteins required a more sensitive MS technique, such as selected reaction monitoring (SRM). This targeted MS method monitors only selected peptides and their fragments in triple-quadrupole mass spectrometers, generating data of high sensitivity and spanning a large dynamic range (greater than four orders of magnitude; Lange *et al.*, 2008). When properly optimized, SRM generates high-quality quantification data with good reproducibility, avoiding the problem of missing data points typical of shotgun MS experiments (Picotti *et al.*, 2009; Soste and Picotti, 2013). These qualities make it especially suitable for the analysis of low-abundance proteins and for studies in which selected target proteins need to be monitored—for example, all subunits of a protein complex (Picotti and Aebersold, 2012).

We implemented a sensitive SILAC-SRM method to analyze 25 target proteins with different cellular abundances in multiple yeast mutants. This approach revealed low levels of ERAD for proteins in wild-type cells. In addition, we studied how the OST complex responded to a change in subunit abundance. On the basis of our findings, we propose a sequence of events for OST complex assembly and also present insights into dynamics of protein complexes in general.

RESULTS

Implementing a sensitive SILAC-SRM method to measure protein degradation

The aim of this study was to analyze the turnover of ER membrane protein complexes in *S. cerevisiae*, with a focus on OST. In addition, we analyzed the SEC translocon, PMT complexes, ER chaperones (Kar2p, Pdi1p), known ERAD substrates (PrA, Pdr5p), and control proteins (Rpl5p, Rps1ap, Ilv5p) that are disposed of slowly (Pratt *et al.*, 2002; Belle *et al.*, 2006; Schwanhausser *et al.*, 2011).

Attempts to monitor all proteins of interest by shotgun MS were unsuccessful because of the low sensitivity of this acquisition method. Therefore we coupled a SILAC chase with SRM acquisition (SILAC-SRM; Figure 1A). Proteins were labeled by culturing the cells in shake flasks with medium containing heavy isotopes of arginine (R_6) and lysine (K_8). Subsequently cells were transferred to medium with light isotopes of arginine and lysine (R_0, K_0). At different time points, cells were collected and lysed, membranes and luminal fractions were collected, and proteins were solubilized and digested with Lys-C and trypsin. At each time point, ratios of heavy to light peptides were recorded by SRM on a QTRAP mass spectrometer (Supplemental Table S1). The rate of protein loss (k_{LOSS}) was calculated by linear curve fitting. Dilution rates (k_{DIL}) by cell division were subtracted from k_{LOSS} to yield degradation rates (k_{DEG}; Larrabee *et al.*, 1980). Using the SILAC-SRM method, we were able to determine degradation rates of 25 target proteins, including eight OST subunits.

To test whether the SILAC-SRM method accurately determined protein half-lives, we used the ERAD model substrate PrA*, a misfolded variant of the PrA glycoprotein (Finger *et al.*, 1993). PrA* has two glycosites, and a glycan on the first site is essential for efficient ERAD. In PrA*-Ab, only the first glycosite is occupied, and in PrA*-aB, only the second one. This influences the rate by which PrA*-Ab and PrA*-aB are degraded via ERAD (fast and slow, respectively; Spear and Ng, 2005). Cells deficient in PrA were transformed with PrA*-aB or PrA*-Ab expression plasmids. SRM traces and degradation rates showed that PrA*-Ab was degraded rapidly, whereas PrA*-aB was more stable (Figure 1, B and C). The obtained values were in agreement with the respective half-lives obtained in classical pulse-chase experiments reported in the literature (Spear and Ng, 2005).

When we overexpressed PrA in wild-type and in ERAD-deficient Δ*hrd1*Δ*doa10* cells, degradation rates of PrA were similar between wild-type and mutated cells. PrA had a half-life of >12 h (or more than eight doubling times; Figure 1D). Thus, within the time in which a given amount of PrA was reduced by a factor 2 via degradation, cell division diluted the same amount by a factor of $2^8 = 256$. Therefore the contribution of degradation to protein turnover was minimal, and, in agreement with previous reports, we classified PrA as "stable" (Finger *et al.*, 1993). From the results of these experiments, we concluded that the SILAC-SRM method was a sensitive and reliable approach for measuring the turnover of proteins and yielded accurate half-lives as compared with previously used methods. Its sensitivity and consistency make SRM especially suitable to analyze medium-to low-abundance proteins (potentially as low as 50 copies/cell), and subunits of protein complexes (Picotti *et al.*, 2009), thus opening many opportunities for applying the method.

Proteins are stable in exponentially growing yeast cells

Next we examined whether and to what extent the ERAD system eliminated other proteins, including subunits of the OST complex, of the SEC translocon complex, and of the PMT complexes, and ER chaperones (Kar2p, Pdi1p; Figure 2A). We conducted pulse-chase experiments in wild-type (ERAD-competent) and Δ*hrd1*Δ*doa10* (ERAD-deficient) cells, isolated membrane and vesicular content fractions, and extracted and digested proteins. Protein turnover for 25 target proteins was analyzed by SRM (Figure 2A). All of these proteins were stable in wild-type cells, and for most proteins, we did not find significant differences in the degradation rates in wild-type cells compared with those observed in Δ*hrd1*Δ*doa10* cells (Figures 2B). In addition, Pmt2p was stable in both cell types, despite having statistically different half-lives ($t_{1/2}$ of 17 vs. 42 h). Thus, in exponentially growing cells, ERAD is of minor importance for homeostasis of the proteins analyzed.

To analyze whether the low level of degradation was a general feature of yeast proteins, we monitored the turnover of proteins from all cellular fractions. To this end, we prepared whole-cell extracts from pulse-chase–labeled wild-type cells by glass bead lysis in detergent. The extracts were processed for mass spectrometry and analyzed by shotgun MS. Half-lives were obtained for 188 proteins from cytosol, mitochondria, nucleus, Golgi, ER, cell wall, and the vacuole. Most of the detected proteins were stable under the culturing conditions used in this study (Figure 2, C and D). Because most of the 25 target proteins we had previously measured using SILAC-SRM were not detected at all or not at all three time points, we were unable to calculate degradation rates. However, we were able to detect Pdi1p, Kar2p, and Rps1ap, which were again stable, as in the SILAC-SRM experiments. Of 188 proteins analyzed, only eight showed half-lives <12 h. This group included proteins that

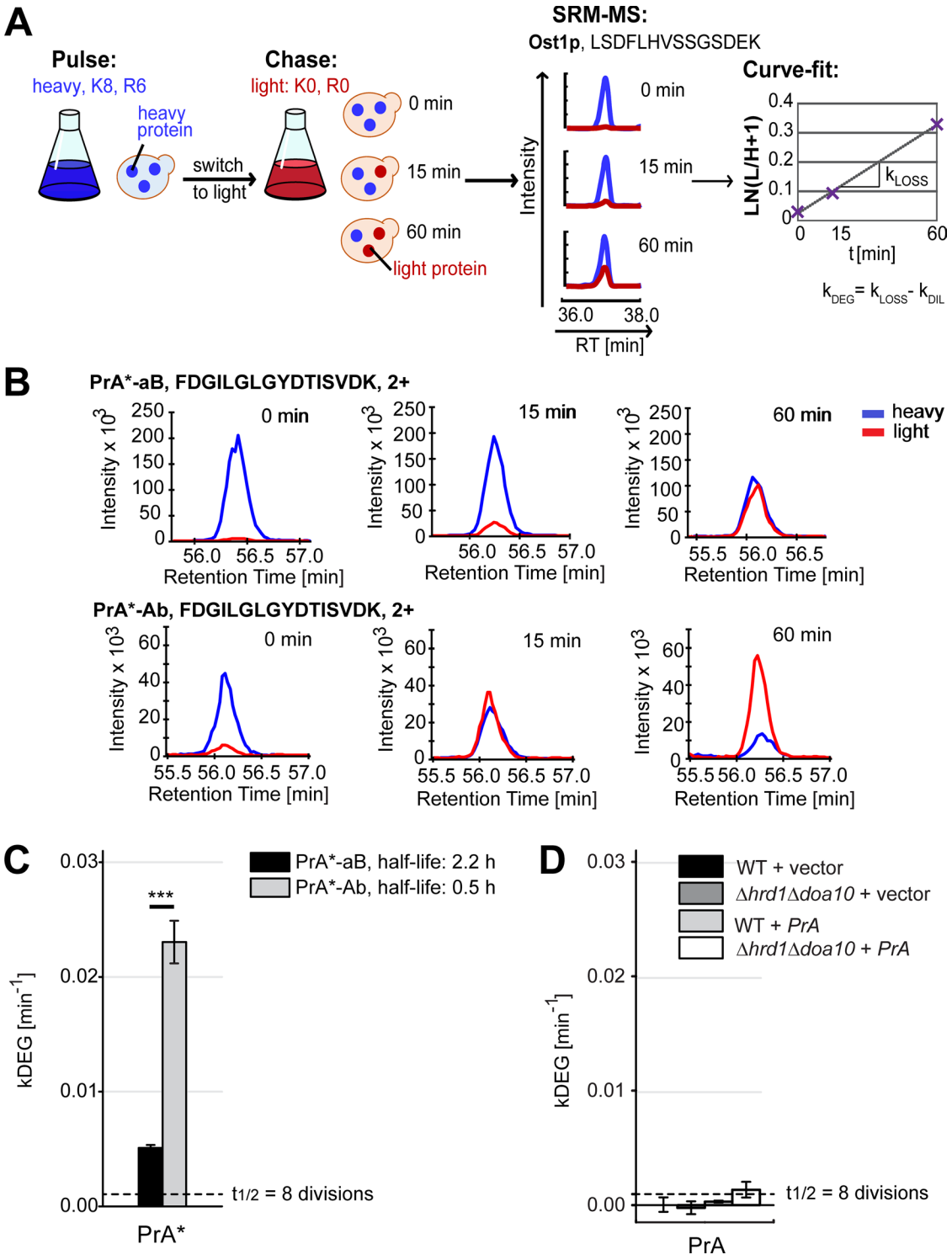

FIGURE 1: Analysis of protein degradation by SILAC-SRM. (A) Schematic representation of the SILAC-SRM method. After labeling of yeast proteins with heavy arginine (R_6) and lysine (K_8), cells were transferred to light medium. Cells were sampled at different time points and proteins prepared for mass spectrometry. Changes in heavy-to-light ratios for peptides were detected by SRM. Loss rates (k_{LOSS}) were calculated by linear curve fitting, and dilution rates (k_{DIL}) corresponding to protein loss through cell division were subtracted, yielding degradation rates (k_{DEG}). (B) Validation of the SILAC-SRM method using PrA. SRM traces for peptide FDGILGLGYDTISVDK of PrA in cells expressing PrA*-aB (SMA822) or PrA*-Ab (SMA823) version of the protein. (C) k_{DEG} values for PrA in cells expressing PrA*-aB (SMA822) or PrA*-Ab (SMA823) version of the protein. Degradation rates were calculated as described in A. Error bars represent SD of three biological replicates. ***$p \leq 0.001$. (D) k_{DEG} values for PrA in wild-type (SMA1648) or *Δhrd1Δdoa10* (SMA1649) cells containing a PrA expression plasmid or vector controls (SMA1574, SMA1584). Degradation rates were calculated as described in A. Error bars represent SD of three biological replicates. The dashed line indicates a half-life of eight cell divisions.

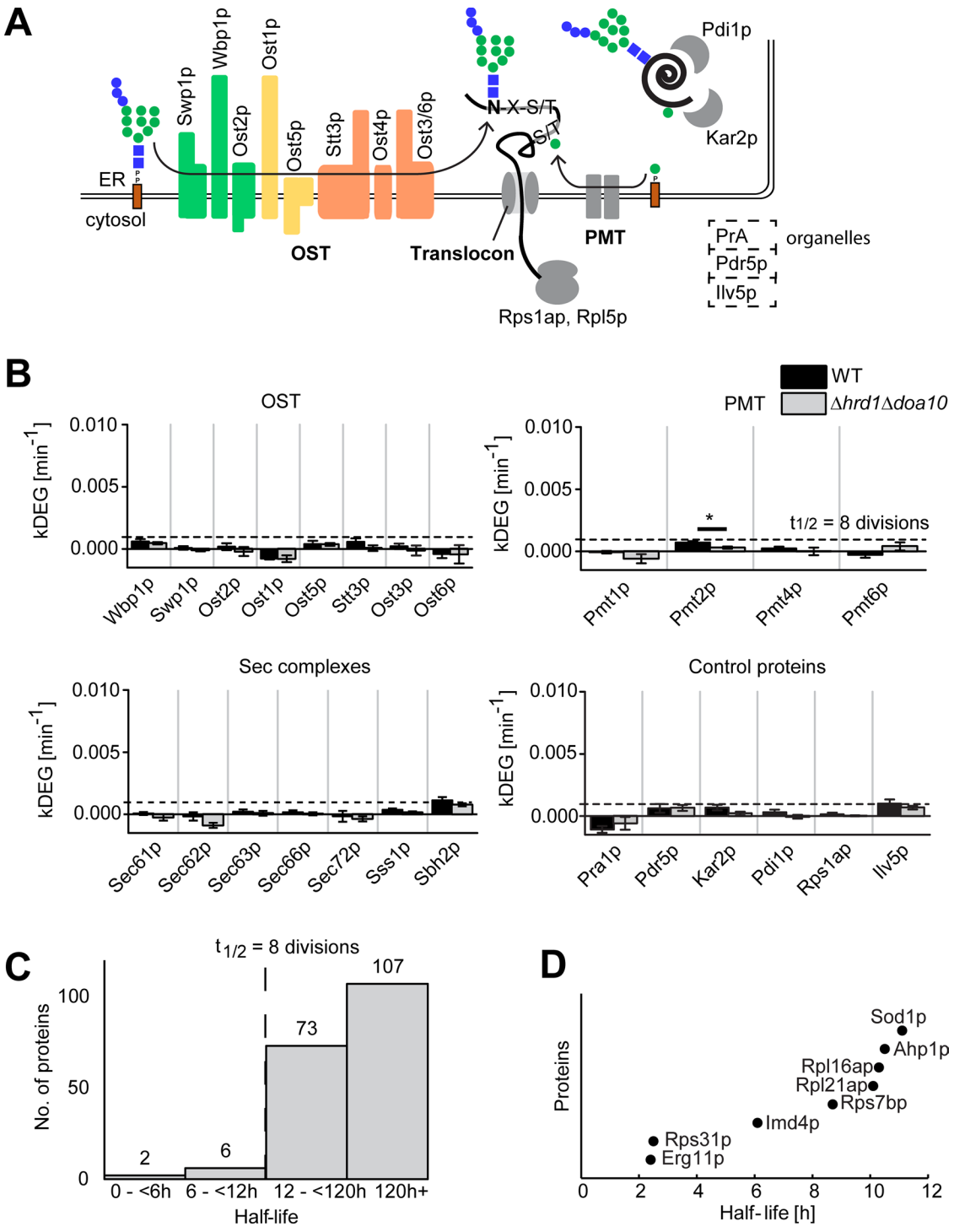

FIGURE 2: Low levels of protein degradation in exponentially growing yeast cells. (A) Schematic representation of target protein localization and function. Proteins are synthesized by ribosomes and enter the ER through the SEC translocon. They are glycosylated by OST (N-glycans) or the PMT complexes (O-glycans). Folding is assisted by chaperones Pdi1p and Kar2p. Further target proteins were the vacuolar protease PrA, the plasma membrane transporter Pdr5p, and the mitochondrial protein Ilv5p. OST subunits are colored green, yellow, or orange according to subcomplexes as proposed previously (Kelleher and Gilmore, 2006). (B) k_{DEG} values for 25 target proteins in wild-type (SMA673) or *Δhrd1Δdoa10* (SMA1566) cells. Degradation rates were measured as described in Figure 1A. Error bars represent SD of three biological replicates. *$p \leq 0.05$. Turnover of Ost4p could not be determined, since tryptic digest yielded only a 35-residue peptide (out of 36 in total), which was too long to be analyzed by MS accurately. (C) Protein half-lives in whole-cell extracts. Whole-cell extracts of wild type (SMA673) were prepared, and proteins were digested for MS and measured by shotgun LC-MSMS and quantified with MaxQuant. Results of three biological replicates. (D) Proteins with half-lives <12 h (average of three biological replicates) from whole-cell extract in C. The dashed line indicates a half-life of eight cell divisions.

cope with oxidative damage (Sod1p, Ahp1p), as well as a known rapidly degrading ribosomal protein (Rps31p) and a protein involved in ergosterol synthesis (Erg11p), a pathway that contains several enzymes whose amount is regulated by degradation (Figure 2, C and D; Hampton and Rine, 1994; Helbig *et al.*, 2011; Jaenicke *et al.*, 2011). From these experiments, we speculated that most proteins were stable in exponentially growing yeast cells under the conditions used in our experiments.

Overexpressed OST subunits are degraded with protein-specific rates

In a next step, we specifically altered protein levels and analyzed the effect of single-subunit overexpression on the turnover of the OST components. Wild-type and Δ*hrd1*Δ*doa10* cells were transformed with a high–copy number plasmid carrying an expression copy of *STT3*. Stt3p is an essential membrane protein and acts as the catalytic subunit of the OST complex, transferring N-glycans onto asparagine residues of proteins. We first analyzed steady-state levels of OST components by SDS–PAGE and immunoblot (Figure 3A). As expected, Stt3p was present in higher amounts in cells containing the overexpression plasmid as compared with the control cells, whereas protein levels remained the same for the other subunits we monitored (Ost1p, Ost3p, and Wbp1p). Analysis of the glycoprotein CPY revealed that glycosylation was not altered upon *STT3* overexpression. The experiment was repeated for all other OST subunits with the same results: overexpression of one subunit did affect the protein levels of the other subunits nor CPY glycosylation (data not shown). We concluded that the OST complex remained intact and functional in the presence of overexpressed subunits.

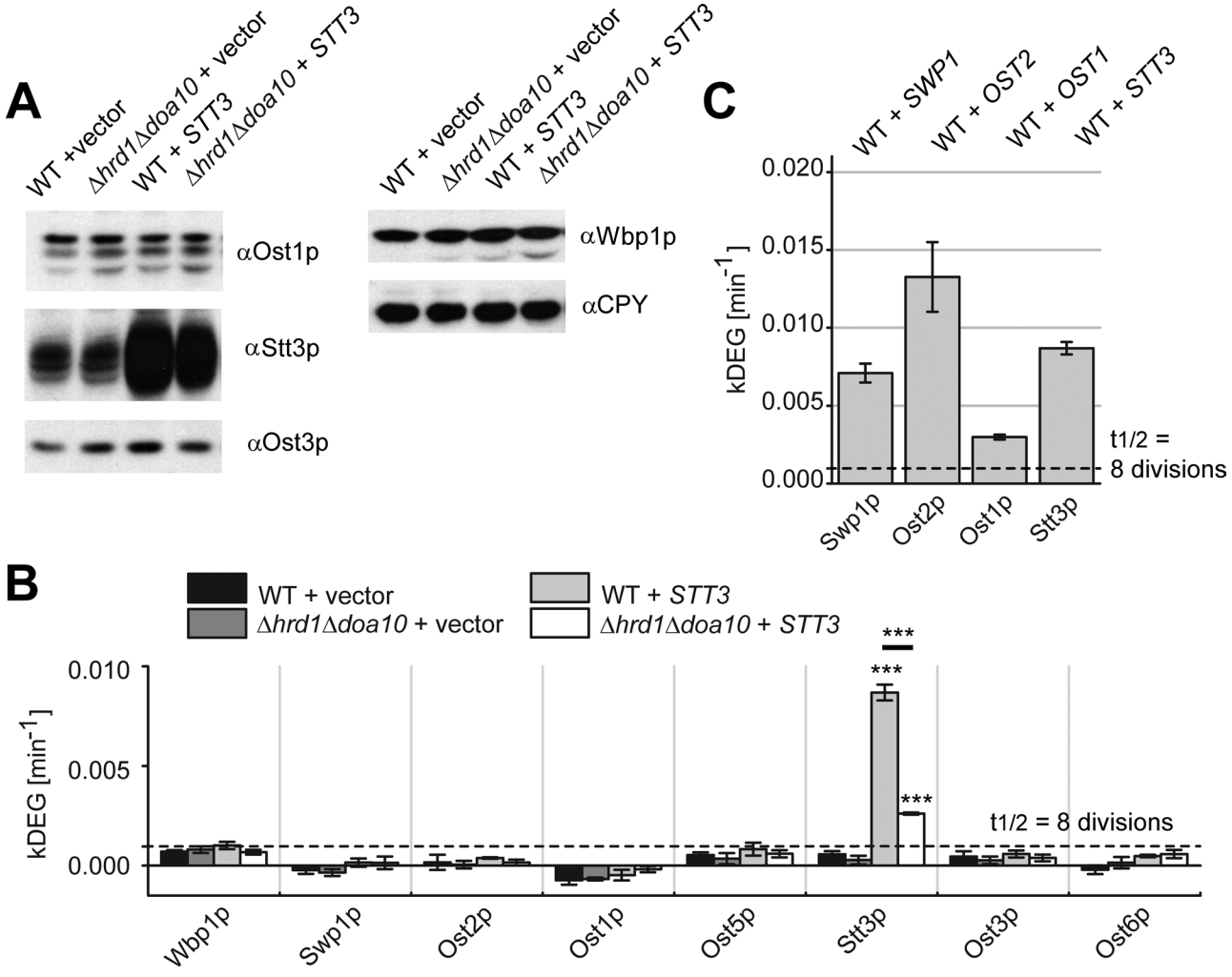

FIGURE 3: Overexpressing OST subunits results in increased degradation. (A) Immunoblot analysis of Stt3p overexpression. SDS extracts were prepared from wild-type (SMA1578) or Δ*hrd1*Δ*doa10* (SMA1588) cells containing a *STT3* expression plasmid and vector controls (SMA1574, SMA1584). Equal amounts of proteins were separated via SDS–PAGE and analyzed by immunoblot with the antibodies indicated. (B) k_{DEG} values for OST subunits in wild-type or Δ*hrd1*Δ*doa10* cells containing either an *STT3* expression plasmid (SMA1578 or SMA1588, respectively) or vector controls (SMA1574 or SMA1584). Degradation rates were measured as described in Figure 1A using SILAC-SRM. Error bars represent SD in three biological replicates. ***$p \leq 0.001$. (C) k_{DEG} values for overexpressed Swp1p (SMA1576), Ost2p (SMA1577), Ost1p (SMA1582), and Stt3p (SMA1578) in ERAD-competent cells. Degradation rates were determined as described in Figure 1A using SILAC-SRM. Error bars represent SD in three biological replicates. The dashed line indicates a half-life of eight cell divisions.

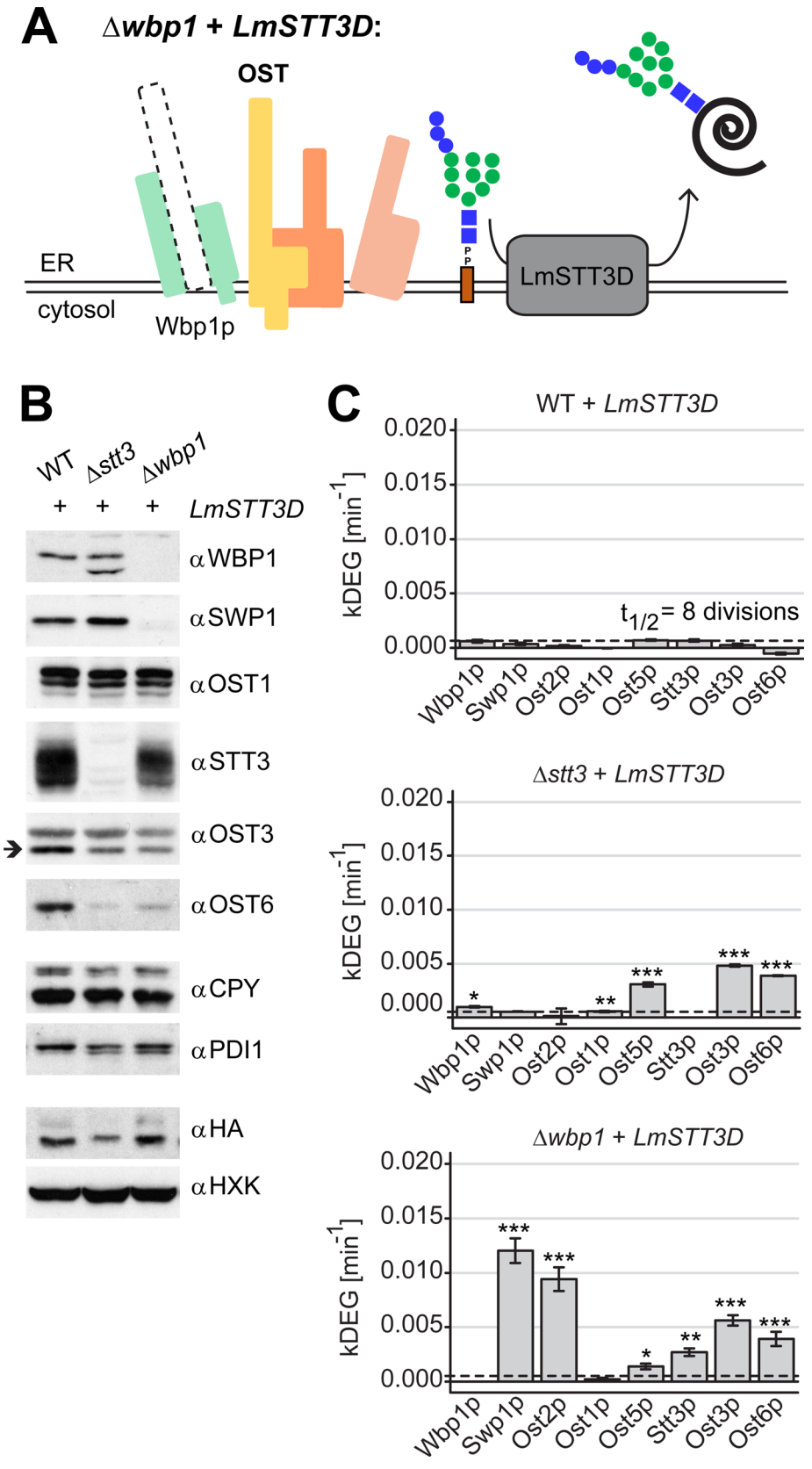

FIGURE 4: Deletion of essential OST subunits affects stability of other complex components. (A) Schematic representation of LmSTT3D compensating N-glycosylation in Δ*wbp1* cells. LmSTT3D glycosylates yeast proteins and ensures cell viability in the absence of a functional yeast OST. (B) Immunoblot analysis of OST deletions. SDS extracts were prepared from cells carrying *LmSTT3D* expression plasmid (hemagglutinin-tagged protein) and containing all OST subunits (wild type, SMA1603) or deletions in *STT3* (SMA1604) or *WBP1* (SMA1605). Equal amounts of protein were separated on a 10% SDS–PAGE gel and transferred to nitrocellulose membranes, followed by detection with specific antibodies. Ost3p signal is indicated by an arrow to distinguish it from unspecific signal. Hexokinase (HXK) was used as loading control. (C) k_{DEG} values for OST subunits in wild type (SMA1603) or in cells deleted in *STT3* (SMA1604) or *WBP1* (SMA1605) and carrying a *LmSTT3D* expression plasmid. Degradation rates were calculated as described in Figure 1A using SILAC-SRM. Error bars represent SD of three biological replicates. *$p \leq 0.05$, **$p \leq 0.01$, ***$p \leq 0.001$. The dashed line indicates a half-life of eight cell divisions.

We then measured degradation rates of overexpressed Stt3p in wild-type and Δ*hrd1*Δ*doa10* cells. Stt3p was stable when present at normal levels (Figure 3B). In contrast, overexpressed Stt3p was degraded at higher rates in wild-type and Δ*hrd1*Δ*doa10* cells, but its half-life was significantly higher in Δ*hrd1*Δ*doa10* (4.4 h) than in wild-type cells (1.3 h), demonstrating that degradation of overexpressed Stt3p depended primarily on a functional ERAD system. All other OST subunits remained stable. Like Stt3p, overexpressed Ost1p, Ost2p, and Swp1p were rapidly degraded in wild-type cells (Figure 3C). Of interest, degradation rates were significantly different for each protein, with half-lives of 3.9 (Ost1p), 0.9 (Ost2p), and 1.5 h (Swp1p; $p < 0.05$). OST subunits that were not overexpressed, on the other hand, remained stable in these strains. Together with previous findings, our data implied that fully assembled OST complexes remained undisturbed, whereas excess subunits were unstable and degraded with protein-specific rates by the ERAD machinery (Jakob *et al.*, 2001). However, it is important to note that overexpression of a protein is not sufficient for protein degradation, as shown for overexpressed PrA (Figure 1D).

Deleting essential subunits destabilizes the OST complex

Our results suggested that integration of OST subunits into the complex prevented their degradation. In a next step, we analyzed the effect of single-subunit deletions on OST component degradation. To study the effect of a deletion of an essential OST subunit, we took advantage of the finding that a plasmid-borne STT3D protein from *Leishmania major* (LmSTT3D) can functionally replace yeast OST (Figure 4, A and C; Nasab *et al.*, 2008). LmSTT3D is a single-subunit oligosaccharyl transferase that glycosylates most proteins when expressed in yeast cells but is not incorporated into the

yeast OST complex. In the presence of LmSTT3D, cells containing a deletion in one of the OST subunits remain fully viable (Figure 4A). Wild-type, Δ*stt3*, and Δ*wbp1* cells carrying the LmSTT3D plasmid were analyzed by SDS–PAGE and immunoblot (Figure 4B). Deletion of Stt3p and Wbp1p had different effects: both resulted in a decrease of Ost3p and Ost6p levels in the presence of overexpressed LmSTT3D, and deleting *WBP1* additionally decreased Swp1p levels. The differences were not caused by LmSTT3D overexpression in wild-type cells, since Ost3p and Ost6p levels were the same in wild-type cells carrying an empty vector or the overexpression plasmid (unpublished data). Whereas CPY was completely glycosylated in Δ*stt3* cells, the Wbp1p subunit was hypoglycosylated, indicating that LmSTT3D fully glycosylated many but not all yeast glycoproteins (Figure 4B).

In a subsequent set of experiments, we measured protein degradation by SILAC-SRM in LmSTT3D-complemented wild-type, Δ*stt3* , and Δ*wbp1* cells. Deletion of both *STT3* and *WBP1* resulted in degradation of several OST subunits but did not affect the SEC and PMT subunits we analyzed (Figure 4C; unpublished data). In Δ*stt3* cells, Ost3p ($t_{1/2}$ = 2.4 h), Ost6p (3.0 h), and Ost5p (3.8 h) were degraded rapidly, and degradation rates of Ost1p ($t_{1/2}$ = 20.2 h) and Wbp1p (11.7 h) were significantly higher than in wild-type cells. In Δ*wbp1* cells, Swp1p ($t_{1/2}$ = 1.0 h), Ost2p (1.2 h), Ost3p (2.1 h), and Ost6p (3.0 h) were degraded. Stt3p ($t_{1/2}$ = 4.4 h) and Ost5p (8.5 h) were also disposed of but with slower rates. We concluded that integration of subunits into the fully assembled complex prevented their degradation; conversely, absence of Stt3p and Wbp1 destabilized other subunits. We speculated that this phenomenon mainly applied to partner proteins of the respective subcomplex or to subunits that entered the complex subsequent to the deleted component.

Study of protein abundances reveals the sequence of events in OST complex assembly

Our results are in line with published data showing that subunits of membrane protein complexes stabilize each other and assemble in a sequential manner via stable intermediates (Daley, 2008). To further elucidate OST assembly, we monitored subunit levels in cells deleted in one of the nine OST subunits using steady-state SILAC-SRM (Figure 5, A and B). Pellets of equal weight of wild-type cells grown in medium with heavy arginine and lysine isotopes and of cells with a deletion in one OST subunit grown in medium with light isotopes were pooled. Both cell types carried the LmSTT3D expression plasmid. Cells were lysed, membranes collected, proteins prepared for MS, and peptides measured by SRM (Figures 5, A and B). Apart from the OST components, we also monitored the behavior of the SEC translocon and PMT subunits, as well as the plasma membrane glycoprotein Pdr5p. With the exception of Pdr5p, most of these proteins showed minor alterations. We concluded that differences reflected the activity of endogenous OST and the LmSTT3D enzyme.

For the OST subunits, we observed a response that was specific for each deletion: A deletion in *WBP1*, *SWP1*, or *OST2* reduced the levels of all these proteins, indicating that the three subunits stabilized each other (Figure 5B). In addition, Wbp1p, Swp1p, and Ost2p were present in similar amounts relative to each other in all other cells, including Δ*ost1* (83–88%) and Δ*stt3* cells (86–92%). We found a similar scenario for *OST1*, *STT3*, and *OST5*: a deletion in *OST1* reduced levels of Stt3p and Ost5p to <20% of wild-type levels. Deletion of *STT3* decreased the protein levels of Ost1p and Ost5p to 68%, whereas a deletion in *OST5* did not affect the levels of any other subunits. Moreover, the three subunits Ost1p, Ost5p, and Stt3p were present in similar amounts relative to each other in all other cells, including Δ*wbp1* (65–83%), Δ*swp1* (72–93%), and Δ*ost2* cells (73–86%). Again, this indicated mutual stabilization of these three subunits. We noted that Ost1p had been stable in SILAC-SRM experiments with Δ*wbp1* cells, but its levels were reduced in steady-state SILAC-SRM experiments with the same cells (Figures 4C and 5B). Thus, determining relative protein levels might be more sensitive and could detect small stability differences that are not visible in pulse-chase experiments. It is possible that the remaining subcomplexes are eventually degraded with very slow kinetics that is not detectable in the SILAC-SRM experiment but becomes evident when analyzing steady-state levels.

In Δ*ost4* cells, levels of only Ost3p and Ost6p were reduced, in agreement with previous findings that Ost4p was necessary for anchoring Ost3p or Ost6p into the OST complex (Spirig *et al.*, 2005). Deletions of *OST3* and *OST6* did not affect the levels of any of the other subunits, whereas levels of Ost3p and Ost6p were reduced upon deletion of any of the other subunits except for Ost5p (Figure 5B). This indicated that Ost3p and Ost6p entered the complex only after all the other subunits had been assembled. Our findings suggested that Wbp1p, Swp1p, and Ost2p on one hand, and Ost1p, Ost5p, and Stt3p on the other hand, formed two subcomplexes that might act as intermediates during complex assembly. Ost4p entered the complex after the two subcomplexes and anchored Ost3p or Ost6p into the OST complex (Spirig *et al.*, 1997, 2005).

ERAD compensates different gene doses in heterozygous diploid yeast cells

To eliminate any LmSTT3D-dependent effects on N-glycosylation, we verified our results by analyzing heterozygous deletions in diploid yeast cells. Because yeast cells do not have a feedback mechanism to control protein levels, deletion of one gene copy in diploid cells decreases the protein level by 50% (Springer *et al.*, 2010; Li *et al.*, 2014). The reduced level of OST activity was still sufficient for the cells to maintain N-glycosylation and survive. We compared protein levels in diploid cells with a heterozygous deletion in *OST1* (Δ*ost1/OST1*) or *WBP1* (Δ*wbp1/WBP1*) to those of diploid wild-type cells. Heterozygous diploid and diploid wild-type cells were cultured in medium containing light or heavy arginine and lysine isotopes. We harvested cells in exponential phase, pooled equal cell weights, and isolated membranes as described. Proteins were extracted and digested, and peptides were quantified using SRM.

Heterozygous deletions of *OST1* and *WBP1* reduced the levels of the respective protein to ~50% relative to wild-type cells (Figure 6). In addition, deletion of *OST1* decreased protein levels of Ost5p, Stt3p, Ost3p, and Ost6p, whereas Wbp1p, Swp1p, and Ost2p levels remained at ~100%. Deletion of *WBP1* reduced the amounts of all other OST subunits. The pattern of subunit reduction was the same as the one observed in haploid cells with a single-subunit deletion and containing the complementing LmSTT3D protein. We conclude that protein degradation is essential for subunit homeostasis of protein complexes, in particular in heterozygous cells.

DISCUSSION

In this study, we combined SILAC and SRM mass spectrometry to measure degradation rates of yeast proteins in exponentially growing yeast cultures using standard laboratory flasks (Figure 1A). The advantage of this method is that many proteins can be analyzed in the same sample, and with assays for the whole yeast proteome at hand, the scale of future studies can be largely extended (Picotti *et al.*, 2013). Using the highly sensitive SRM acquisition method enabled recording of degradation rates of intermediate- to low-abundance proteins that are not detectable by SILAC shotgun MS approaches,

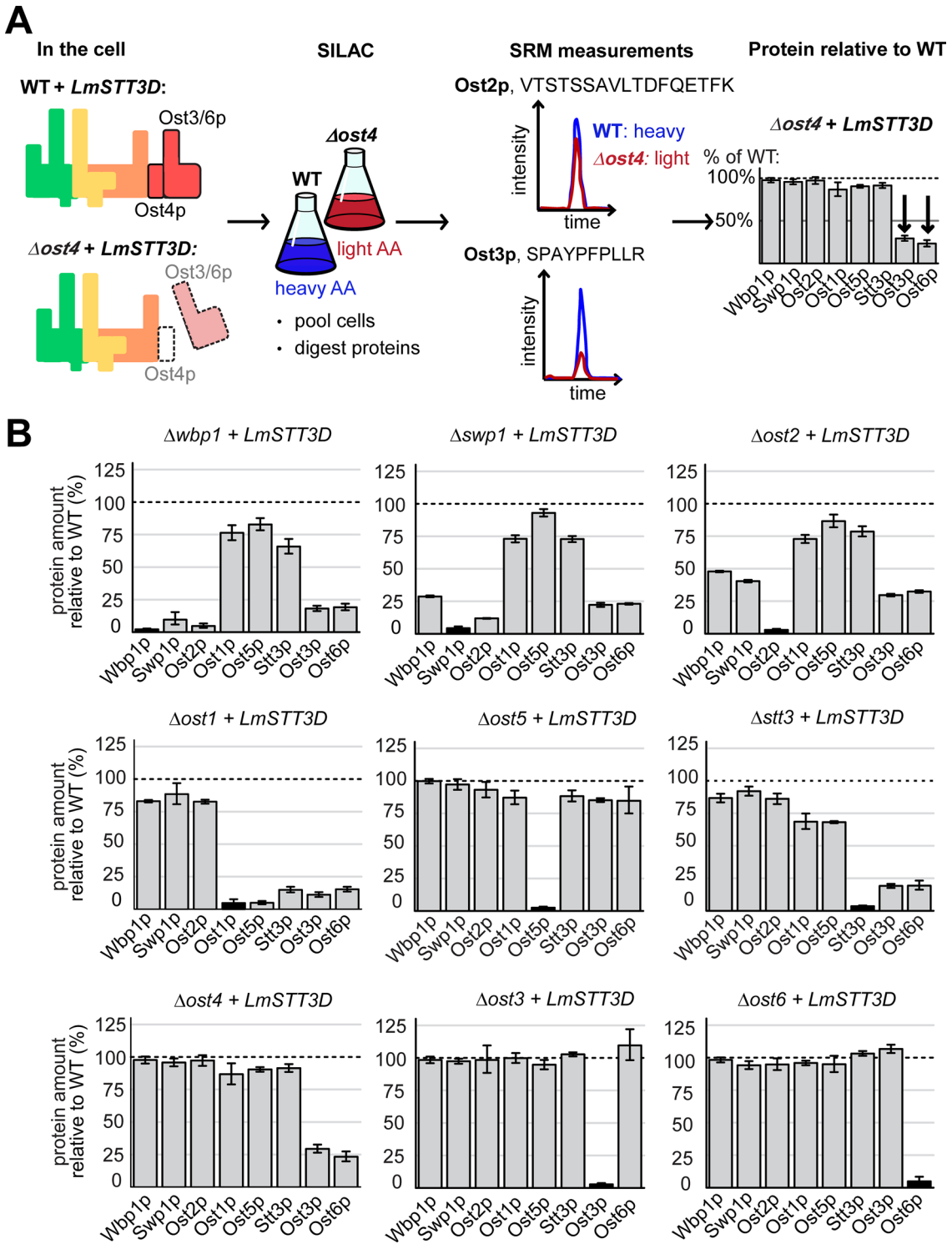

FIGURE 5: Differential effect of subunit deletion on OST component stability. (A) Schematic representation for SILAC analysis of cells with an OST subunit deletion. LmSTT3D-complemented wild type and cells with a subunit deletion (Δ*ost4*) were grown in medium containing heavy (WT) or light (Δ*ost4*) amino acids. Equal amounts of cells were pooled, proteins were extracted, and peptides were prepared for mass spectrometry. Light-to-heavy ratios for all OST peptides were measured by SRM. Subunit abundance relative to wild type was calculated. Values were normalized to the average of all non-OST proteins. Decreased amounts of a subunit, as for Ost3p and Ost6p, indicated its destabilization by the Δ*ost4* deletion. (B) Amounts of OST components relative to wild type (SMA1603 or SMA1651) in cells deleted in a single subunit and containing an *LmSTT3D* expression plasmid (SMA1604-1609, YG2073, YG2075, YG2080) were analyzed as described in A. The values were normalized by dividing by the average of all non-OST proteins (SEC, PMT components, Pdr5p). Except for deletion of OST4, a black bar indicates the abundance of the deleted subunit that is produced by background signal during SRM measurements. Error bars represent the 95% confidence interval of the average of three biological replicates.

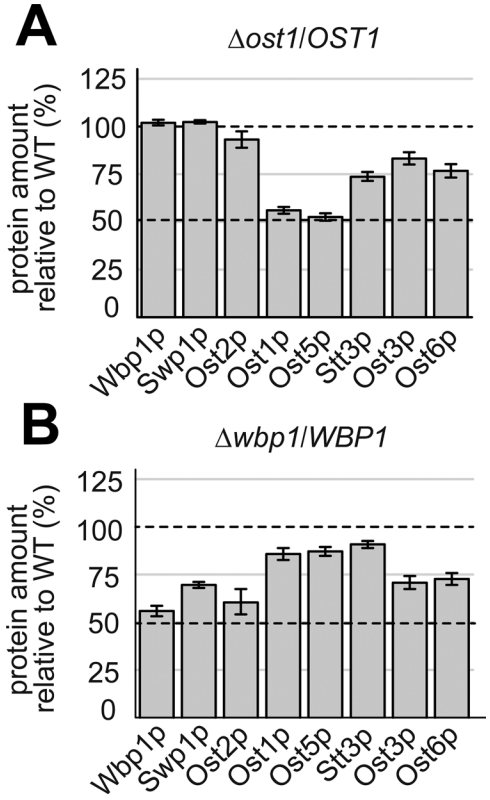

FIGURE 6: Gene dosage of OST components affects subunit stability in diploid yeast cells. Cells with a heterozygous subunit deletion (Δ*ost1/OST1* = SMA1621, Δ*wbp1/WBP1* = SMA1628) were grown in medium containing light amino acids (R_0, K_0). In parallel, wild-type cells (SMA1620) were grown in medium containing heavy amino acids (R_6, K_8). Equal weights of cells grown in heavy and light media were pooled, proteins were extracted, and peptides were prepared for mass spectrometry. Light-to-heavy ratios for all OST peptides were measured by SRM. Subunit abundance relative to wild type was calculated and normalized to the ribosomal protein Rpl5p. Subunit levels relative to wild-type cells grown in heavy medium are displayed for Δ*ost1/OST1* cells (A) and Δ*wbp1/WBP1* cells (B). Averages of three biological replicates. Error bars indicate the 95% confidence interval.

potentially down to 50 copies/cell (Picotti *et al*., 2009). Moreover, the reproducible and consistent data obtained with SRM are especially beneficial in pulse-chase experiments in which a defined set of peptides is monitored over several time points. In contrast to data-dependent MS experiments, in which missing data points are common due to varying peak intensities and coelution of peptides, the number of data points collected over each eluting peptide is much higher, which results in more accurate data for quantification. In summary, we demonstrate that the SILAC-SRM approach is a sensitive and reliable method for measuring degradation rates of medium-to low-abundance proteins and for monitoring protein complex stability.

We measured yeast protein half-lives over a time range from 20 min to many hours. Most proteins in wild-type yeast cells had very low degradation rates and half-lives >12 h (Figure 2, B and C). Only a small number of proteins showed half-lives <12 h, and these findings are in agreement with previous results from yeast showing that the analyzed wild-type proteins were stable (Futcher *et al*., 1999; Xie *et al*., 2009). In addition, two studies using SILAC coupled to shotgun MS reported long average or median protein half-lives of 32 and 11 h in yeast chemostat cultures grown under nutrient limitation (Pratt *et al*., 2002; Helbig *et al*., 2011). Low protein degradation levels or long median half-lives (ranging from 2 to 9 d) were also found for other species, including *Escherichia coli*, mouse fibroblasts, and mouse brain cells (Larrabee *et al*., 1980; Price *et al*., 2010; Schwanhausser *et al*., 2011). Together these findings imply that protein homeostasis is mainly regulated via synthesis. Indeed, two recent studies showed that in *E. coli* and mammalian cells, protein abundance is mainly controlled at the level of translation, minimizing the need for degradation of excess protein (Schwanhausser *et al*., 2011; Li *et al*., 2014). The absence of degradation is of specific importance for protein complexes and implies that synthesis rates correlated to subunit stoichiometry. Indeed, a recent study (Li *et al*., 2014) and our results confirm this hypothesis.

Nevertheless, the ERAD system is set in place to degrade excess subunits, as we show for overexpressed OST subunits (Figure 3, B and C). The finding that subunits were disposed of with protein-specific rates could be explained by protein-specific interactions with the ERAD machinery. Deleting essential OST subunits, on the other hand, destabilized the complex and resulted in subunit degradation (Figure 4C). This suggests that in the absence of their binding partners, subunits might be thermodynamically instable or expose degradation signals targeting them for ERAD. We therefore suggest that OST is destabilized by subunit deletion but not overexpression and that this principle might apply to many yeast protein complexes. Such "cooperative stability" has been described for several heteromeric and homomeric complexes in yeast and other organisms (Johnson *et al*., 1998; Asher *et al*., 2006; Daley, 2008). In agreement with this scenario, overexpressed single subunits of protein complexes were degraded in aneuploid yeast cells (Dephoure *et al*., 2014). This complex stability model also implies that protein complex function is robust in the face of large-scale gene duplications, since overexpression of a single subunit does not affect enzyme activity and simultaneous duplication of all subunit loci is unlikely. Therefore organizing enzymes as complexes ensures constant activity of key processes, such as N-glycosylation or protein synthesis, irrespective of aneuploidy or heterozygosity.

We quantified relative subunit levels in cells deleted in one of the OST subunits relative to wild type and deduced a sequence of events for the assembly of the OST complex (Figures 6B and 7). In agreement with previous studies, Wbp1p, Swp1p, and Ost2p form one subcomplex (subcomplex 1 in Figure 7; Silberstein *et al*., 1995; Karaoglu *et al*., 1997; Kelleher and Gilmore, 1997; Spirig *et al*., 1997). Similarly, Ost1p and Ost5p bind to each other and form another subcomplex together with Stt3p (subcomplexes 2a and 2b). Previous studies showed genetic and biochemical interactions of Ost1p and Ost5p and suggested that these proteins form a subcomplex (Reiss *et al*., 1997; Yan *et al*., 2003). However, since a deletion of Ost5p rendered neither Ost1p nor Stt3p instable, it is possible that Ost5p is of minor importance to the stability of this subcomplex and constitutes an auxiliary subunit (Figure 5B). In a next step, subcomplexes 1 and 2 interact to form the next assembly intermediate. Subsequently Ost4p binds to Stt3p and anchors Ost3p or Ost6p into the OST complex (Spirig *et al*., 1997, 2005). Compared to previous studies, this model extends our knowledge on OST architecture and contradicts a proposed Stt3p-Ost4p-Ost3p/Ost6p subcomplex (te Heesen *et al*., 1993; Karaoglu *et al*., 1997; Reiss *et al*., 1997; Spirig *et al*., 1997, 2005; Schwarz *et al*., 2005; Nasab *et al*., 2008). Based on our results, the observed subcomplexes are assembly intermediates that have lower stability than fully assembled OST but confer stability to subunit monomers. Apart from their enzymatic properties, an essential function of the OST subunits is to contribute to complex stability. This property has to be taken into account when reverse genetic tools are used for functional studies.

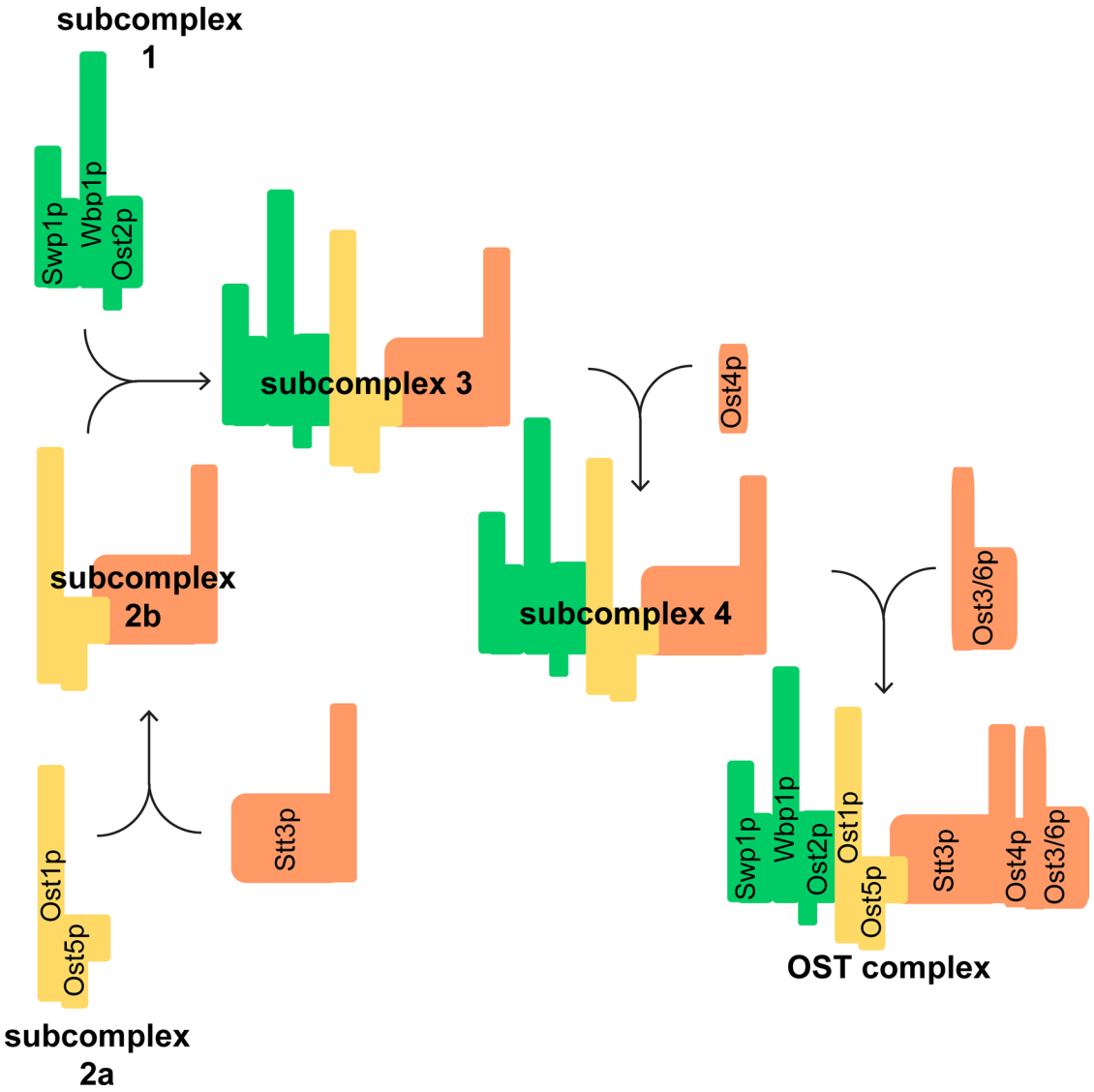

FIGURE 7: Model for OST subcomplexes and complex assembly. Wbp1p, Ost3p, and Swp1p form subcomplex 1. Ost1p is stabilized by Ost5p and forms subcomplex 2 with Stt3p. Together with Ost4p, the two subcomplexes form subcomplex 3. Ost4p then anchors Ost3p or Ost6p into the final complex. Subunits are colored green, yellow, or orange according to Kelleher and Gilmore (2006). Graphical arrangements do not reflect actual interaction sites between subunits.

If most cellular proteins are stable and general turnover is very low, what is the function of ERAD in yeast cells? Clearly, ERAD is essential to dispose of misfolded proteins. In addition, our findings suggest that ERAD adjusts levels of proteins that are unstable because of stoichiometric imbalance, preventing their aggregation. Protein imbalances can be transient because of altered growth conditions (e.g., exponential growth vs. growth under carbon-limiting conditions), and ERAD becomes essential under these conditions. Indeed, expression of ERAD components is increased upon external and internal stress signals (Travers *et al.*, 2000). Constitutive protein imbalance can result from genetic events such as gene duplication or heterozygosity (Chang *et al.*, 2013; Magadum *et al.*, 2013). Under these conditions, protein degradation is crucial to maintain cell survival (Torres *et al.*, 2007, 2010; Dephoure *et al.*, 2014). Of interest, such genetic alterations are the basis for the evolution of novel properties; this would not be possible without a mechanism that regulates protein homeostasis by degradation.

MATERIALS AND METHODS

Reagents

Antibodies used in the study are listed in Supplemental Table S2. The $^{13}C_6$ arginine was from the Cambridge Isotope Laboratories, Tewksbury, MA; $^{13}C_6$-$^{15}N_2$ lysine was from Sigma-Aldrich, St. Louis, MO.

Plasmids and yeast strains

Plasmids used in this study are listed in Supplemental Table S3. The plasmids were constructed using standard cloning protocols.

pPrA: The *PEP4* open reading frame (ORF) and its native promoter and terminator regions were excised from *PEP4*-pRS316 by restriction digest with *Sal*I and *Bam*HI. The DNA fragment was ligated into *Sal*I/*Bam*HI-digested YEp352.

pLmSTT3D-URA: pRS426-GPD-LmSTT3D was digested with *Sac*I and *Eco*RV to obtain a DNA fragment that included the GPD promoter, the Lm*STT3D* ORF, and a *CYC1* terminator region. The DNA fragment was ligated into *Sac*I/*Eco*RV-digested YEp352.

Standard yeast genetic techniques were used (Guthrie and Fink, 1991; Wach *et al.*, 1994; Guldener *et al.*, 1996). Yeast strains used in this study are listed in Supplemental Table S4.

Immunoblot analysis

Cultures were grown in appropriate synthetic drop-out (SD) media to exponential phase. Cells were lysed with glass beads in sample buffer (2% SDS, 62.5 mM Tris/HCl, pH 6.8, 10% glycerol, 6 M urea, 5% β-mercaptoethanol, 0.02% bromophenol blue, protease inhibitor [Complete; Roche], 5 mM phenylmethylsulfonyl fluoride, 25 mM EDTA) by vortexing at 4°C for 15 min. Proteins were dissolved at 37°C for 20 min. Equal amounts of protein were loaded on 10% polyacryl amide gels. Proteins were blotted onto a nitrocellulose membrane. The membrane was hybridized with a primary antibody, washed, and hybridized with appropriate secondary antibodies. Proteins were detected with ECL solution (GE Healthcare, Amersham) and light-sensitive films (Super RX, Fuji Medical X-Ray Film; Fuji, Tokyo, Japan).

SILAC chase experiment

Yeast cells were grown to exponential phase ($OD_{600} = 1$) in appropriate SD medium supplemented with 20 mg/l heavy isotopes of arginine ($^{13}C_6$) and lysine ($^{13}C_6$-$^{15}N_2$). Cells were collected by filtration, washed with SD medium without arginine and lysine, and resuspended in SD medium containing light isotopes of arginine and lysine to obtain $OD_{600} = 0.5$. At the indicated time points, 50 OD of cells were collected, frozen in liquid nitrogen, and stored at –80°C.

Sample preparation for mass spectrometry

Cells were lysed with glass beads in 2 M NaCl, 10 mM 4-(2-hydroxyethyl)-1-piperazineethanesulfonic acid (HEPES)/NaOH, pH 7.4, 1 mM EDTA, and protease inhibitors (Complete; Roche Diagnostics International AG, Rotkreuz, Switzerland) at 4°C for 15 min. The lysate was cleared (1000 × *g*, 5 min), and microsomal fractions were collected by centrifugation at 16,000 × *g* and 4°C for 20 min. Microsomes were resuspended by douncing and sonication in 1 ml of 0.1 M Na_2CO_3 and 1 mM EDTA, pH 11.3, and incubation at 4°C for 30 min. Microsomes were pelleted and separated from the supernatant. A 500-µl amount of the supernatant was precipitated with 55 µl of trichloroacetic acid on ice for 5 min, and pellets were washed two times with acetone. Microsomes were washed once with 1 ml 5 M urea, 100 mM NaCl, 10 mM HEPES, pH 7.4, and 1 mM EDTA and twice with 1 ml 0.1 M Tris/HCl, pH 7.6. Finally, all samples were solubilized in 100–200 µl of 4% SDS, 50 mM dithiothreitol (DTT), and 0.1 M Tris/HCl, pH 7.6, and the solution was cleared by centrifugation.

Proteins were processed using the filter-assisted sample preparation protocol (Wisniewski *et al.*, 2009). Samples were diluted 20-fold with UA buffer (8 M urea, 0.1 M Tris/HCl, pH 8.5) and applied to a 30-kDa cutoff filter device (Amicon; Millipore, Billerica, MA). After washing with 0.4 ml UA, proteins were alkylated in 0.2 ml of 50 mM iodoacetamide for 30 min in the dark. Proteins were washed three times with 0.4 ml UB (8 M urea, 0.1 M Tris/HCl, pH 8.0) and resuspended in 60 µl UB. Proteins were digested with 2 µg of endoproteinase Lys-C (Wako Pure Chemical, Richmond, VA) for 16 h, diluted with 400 µl of 40 mM $NaHCO_3$, and digested with 2 µg of trypsin at 37°C for 4 h. Peptides were eluted, and peptide concentration was determined. A 5-µg amount of peptides was diluted to a final concentration of 3% acetonitrile and pH 2–3 with trifluoroacetic acid. Finally, samples were desalted using C18 ZipTips (Millipore).

SRM assay development

Proteotypic peptides were selected for 26 proteins (including the 25 target proteins and the Rpl5p protein) using BLAST and PeptideAtlas. The majority of transitions (66 of 83 target peptides) were extracted from SRM-atlas using the yeast spectral library build "201207_QQQ_lib.tgz" described by Picotti *et al.* (2013). For the other peptides, we used ions from QTRAP or LTQ Orbitrap runs or theoretical transitions. Retention times were determined by unscheduled SRM runs or were transferred from earlier LTQ Orbitrap runs using Biognosys iRT peptides and linear extrapolation. Several peptides per protein and up to 10 transitions/precursor were analyzed. All peaks were manually inspected for correct assignment and accurate peak integration. The precursor peak was identified by coelution of the transitions, corresponding peptide abundances, relative fragment intensities of light and heavy precursors in SILAC samples, and retention time and comparison to the spectral library (dot product >0.7; Picotti *et al.*, 2013). The four or five transitions showing most-intense signals, highest selectivity, and least background or interference for each precursor were selected for the final method. For the 25 target proteins and Rpl5p, we assembled a list of 83 peptides and 982 transitions (Supplemental Table S1). For 43 peptides, transitions were validated using synthetic peptides (SpikeTides; JPT, Berlin, Germany). In addition, transitions for some peptides were tested by measuring yeast cells in which the corresponding protein was overexpressed or absent due to a deletion (Supplemental Table S1).

SRM mass spectrometry

Retention time iRT peptides (Biognosys, Schlieren, Switzerland) were added to all samples in ratios of 1:20–1:40. For each sample, 2–8 µl was injected onto a nano-frit column (15 cm × 75 µm; OD 375 µm; beads, Magic C18 AQ, 3 µm, 200 Å; Bischoff Chromatography, Leonberg, Germany) connected to a spray tip (PicoTip emitter, FS360-20-10-N-20-C12; New Objective; MS Wil, Wil, Switzerland) coupled to an Eksigent nanoLC-Ultra 1D plus (ABSciex, Zug, Switzerland). The column was kept at 50°C. Peptides were eluted using a gradient from 3 to 35% acetonitrile, 0.1% formic acid in water for 57.5 min, and a flow rate of 500 nl/min.

Targeted SRM analysis was performed on a QTRAP 5500 (AB Sciex) equipped with a nanospray ion source. Scheduled SRM runs were performed in positive-ion mode. Interface temperature was 170°C, ion spray voltage was 2000–2500 V, ion source gas pressure was 6–10 psi, curtain gas pressure was 25 psi, and collision gas was set to high. Declustering potential had a value of 100, collision cell exit potential of 13, and entrance potential of 10. Further settings were unit resolution for both Q1 and Q3 and 2-ms pause between mass ranges, 5-min retention time windows for the transitions, and a target scan time of 3 s. Results from scheduled SRM runs were exported to Skyline, and peaks were integrated (MacLean *et al.*, 2010). The peaks were manually inspected for correct assignment and accurate peak integration.

Calculation of protein degradation rates

The loss rate of old protein from the cell (k_{LOSS}) was calculated from the time course of isotopic ratios according to Larrabee *et al.* (1980). Values were normalized to the dilution of protein content by cell division. This was done by subtraction of k_{DIL} (= k_{LOSS} of the stable reference protein Rpl5p). Finally, half-lives were calculated as $t_{1/2} = \ln(2)/k_{DEG}$.

Preparation of whole-cell extracts and shotgun mass spectrometry analysis

An equivalent of 50 OD cells was lysed with glass beads in 100 mM Tris-HCl, pH 7.6, 50 mM DTT, and 4% SDS. Lysates were cleared,

and DNA was sheared by sonication. A 200-µg amount of protein was diluted with 400 µl of UA buffer (8 M urea in 0.1 M Tris-HCl, pH 8.5) and prepared for mass spectrometry as described. Biognosys iRT retention time peptides were added to samples in a 1:40 ratio. A 4-µl amount was analyzed on an LTQ Orbitrap Velos (Thermo Scientific, Bremen, Germany) using reversed-phase liquid chromatography with a water/acetonitrile gradient of 1–35% acetonitrile at the flow rate of 250 nl/min. Runs were acquired running a standard liquid chromatography–tandem mass spectrometry (LC-MS/MS) program of one survey (Fourier transform-MS) scan, followed by 20 ion trap data–dependent scans (MS/MS) looped throughout the run. The survey scans (300–1700 *m/z*) were acquired in profile mode at a resolution of 60,000 at 400 *m/z*. Collision-induced dissociation fragmentation was performed using a normalized collision energy of 35, activation energy of 0.25, and activation time of 10 ms. A 90-s dynamic exclusion was applied with a list size of maximum 500 entries. Peptides were quantified and proteins identified using MaxQuant software (Cox and Mann, 2008).

Steady-state SILAC-SRM experiment

Equal weights of wild-type cells grown in heavy and mutant cells in light medium were mixed in a ratio of 1:1. Samples were prepared, and light (L) and heavy (H) precursor signals were measured by SRM as described. L/H ratios were calculated for each peptide. The amount of OST subunits relative to wild type was calculated from the average L/H over all peptides of a protein. Values were normalized by dividing by the ribosomal control protein Rpl5p or by the average L/H of all non-OST proteins (SEC, PMT proteins, and Pdr5p) of each replicate.

ACKNOWLEDGMENTS

We thank Ramon Sieber, Lisa Rüegg, and Anja Tobler for excellent technical assistance. We thank Paolo Nanni for comments on the manuscript and Jonas Grossmann for advice on statistics. We further thank the Functional Genomic Center Zurich for instrument and personal support. This work was supported by ETH Research Grant No. 07 10-1 to R.G. and M.A. and Swiss National Science Foundation Grant 31003A_127098 to M.A.

REFERENCES

Asher G, Reuven N, Shaul Y (2006). 20S proteasomes and protein degradation "by default." BioEssays 28, 844–849.

Belle A, Tanay A, Bitincka L, Shamir R, O'Shea EK (2006). Quantification of protein half-lives in the budding yeast proteome. Proc Natl Acad Sci USA 103, 13004–13009.

Breitling J, Aebi M (2013). N-linked protein glycosylation in the endoplasmic reticulum. Cold Spring Harb Perspect Biol 5, a013359.

Chang SL, Lai HY, Tung SY, Leu JY (2013). Dynamic large-scale chromosomal rearrangements fuel rapid adaptation in yeast populations. PLoS Genet 9, e1003232.

Cox J, Mann M (2008). MaxQuant enables high peptide identification rates, individualized p.p.b.-range mass accuracies and proteome-wide protein quantification. Nat Biotechnol 26, 1367–1372.

Daley DO (2008). The assembly of membrane proteins into complexes. Curr Opin Struct Biol 18, 420–424.

Dephoure N, Hwang S, O'Sullivan C, Dodgson SE, Gygi SP, Amon A, Torres EM (2014). Quantitative proteomic analysis reveals posttranslational responses to aneuploidy in yeast. Elife 2014, e03023.

Duijf PH, Benezra R (2013). The cancer biology of whole-chromosome instability. Oncogene 32, 4727–4736.

Finger A, Knop M, Wolf DH (1993). Analysis of 2 mutated vacuolar proteins reveals a degradation pathway in the endoplasmic-reticulum or a related compartment of yeast. Eur J Biochem 218, 565–574.

Futcher B, Latter GI, Monardo P, McLaughlin CS, Garrels JI (1999). A sampling of the yeast proteome. Mol Cell Biol 19, 7357–7368.

Guldener U, Heck S, Fiedler T, Beinhauer J, Hegemann JH (1996). A new efficient gene disruption cassette for repeated use in budding yeast. Nucleic Acids Res 24, 2519–2524.

Guthrie C, Fink GR (1991). Guide to Yeast Genetics and Molecular Biology, San Diego, CA: Academic Press.

Gygi SP, Rochon Y, Franza BR, Aebersold R (1999). Correlation between protein and mRNA abundance in yeast. Mol Cell Biol 19, 1720–1730.

Hampton RY, Rine J (1994). Regulated degradation of HMG-CoA reductase, an integral membrane protein of the endoplasmic reticulum, in yeast. J Cell Biol 125, 299–312.

Helbig AO, Daran-Lapujade P, van Maris AJ, de Hulster EA, de Ridder D, Pronk JT, Heck AJ, Slijper M (2011). The diversity of protein turnover and abundance under nitrogen-limited steady-state conditions in Saccharomyces cerevisiae. Mol Biosyst 7, 3316–3326.

Jaenicke LA, Brendebach H, Selbach M, Hirsch C (2011). Yos9p assists in the degradation of certain nonglycosylated proteins from the endoplasmic reticulum. Mol Biol Cell 22, 2937–2945.

Jakob CA, Bodmer D, Spirig U, Battig P, Marcil A, Dignard D, Bergeron JJ, Thomas DY, Aebi M (2011). Htm1p, a mannosidase-like protein, is involved in glycoprotein degradation in yeast. EMBO Rep 2, 423–430.

Johnson PR, Swanson R, Rakhilina L, Hochstrasser M (1998). Degradation signal masking by heterodimerization of MATalpha2 and MATa1 blocks their mutual destruction by the ubiquitin-proteasome pathway. Cell 94, 217–227.

Karaoglu D, Kelleher DJ, Gilmore R (1997). The highly conserved Stt3 protein is a subunit of the yeast oligosaccharyltransferase and forms a subcomplex with Ost3p and Ost4p. J Biol Chem 272, 32513–32520.

Kelleher DJ, Gilmore R (1997). DAD1, the defender against apoptotic cell death, is a subunit of the mammalian oligosaccharyltransferase. Proc Natl Acad Sci USA 94, 4994–4999.

Kelleher DJ, Gilmore R (2006). An evolving view of the eukaryotic oligosaccharyltransferase. Glycobiology 16, 47R-62R.

Lange V, Picotti P, Domon B, Aebersold R (2008). Selected reaction monitoring for quantitative proteomics: a tutorial. Mol Syst Biol 4, 222.

Larrabee KL, Phillips JO, Williams GJ, Larrabee AR (1980). The relative rates of protein synthesis and degradation in a growing culture of Escherichia coli. J Biol Chem 255, 4125–4130.

Lecker SH, Goldberg AL, Mitch WE (2006). Protein degradation by the ubiquitin-proteasome pathway in normal and disease states. J Am Soc Nephrol 17, 1807–1819.

Li GW, Burkhardt D, Gross C, Weissman JS (2014). Quantifying absolute protein synthesis rates reveals principles underlying allocation of cellular resources. Cell 157, 624–635.

MacLean B, Tomazela DM, Shulman N, Chambers M, Finney GL, Frewen B, Kern R, Tabb DL, Liebler DC, MacCoss MJ (2010). Skyline: an open source document editor for creating and analyzing targeted proteomics experiments. Bioinformatics 26, 966–968.

Magadum S, Banerjee U, Murugan P, Gangapur D, Ravikesavan R (2013). Gene duplication as a major force in evolution. J Genet 92, 155–161.

Nasab FP, Schulz BL, Gamarro F, Parodi AJ, Aebi M (2008). All in one: Leishmania major STT3 proteins substitute for the whole oligosaccharyltransferase complex in Saccharomyces cerevisiae. Mol Biol Cell 19, 3758–3768.

Oromendia AB, Amon A (2014). Aneuploidy: implications for protein homeostasis and disease. Dis Model Mech 7, 15–20.

Oromendia AB, Dodgson SE, Amon A (2012). Aneuploidy causes proteotoxic stress in yeast. Genes Dev 26, 2696–2708.

Picotti P, Aebersold R (2012). Selected reaction monitoring-based proteomics: workflows, potential, pitfalls and future directions. Nat Methods 9, 555–566.

Picotti P, Bodenmiller B, Mueller LN, Domon B, Aebersold R (2009). Full dynamic range proteome analysis of S. cerevisiae by targeted proteomics. Cell 138, 795–806.

Picotti P, Clement-Ziza M, Lam H, Campbell DS, Schmidt A, Deutsch EW, Rost H, Sun Z, Rinner O, Reiter L, *et al.* (2013). A complete mass-spectrometric map of the yeast proteome applied to quantitative trait analysis. Nature 494, 266–270.

Pratt JM, Petty J, Riba-Garcia I, Robertson DH, Gaskell SJ, Oliver SG, Beynon RJ (2002). Dynamics of protein turnover, a missing dimension in proteomics. Mol Cell Proteomics 1, 579–591.

Price JC, Guan S, Burlingame A, Prusiner SB, Ghaemmaghami S (2010). Analysis of proteome dynamics in the mouse brain. Proc Natl Acad Sci USA 107, 14508–14513.

Reiss G, te Heesen S, Gilmore R, Zufferey R, Aebi M (1997). A specific screen for oligosaccharyltransferase mutations identifies the 9 kDa OST5 protein required for optimal activity in vivo and in vitro. EMBO J 16, 1164–1172.

Ruggiano A, Foresti O, Carvalho P (2014). Quality control: ER-associated degradation: protein quality control and beyond. J Cell Biol 204, 869–879.
Schwanhausser B, Busse D, Li N, Dittmar G, Schuchhardt J, Wolf J, Chen W, Selbach M (2011). Global quantification of mammalian gene expression control. Nature 473, 337–342.
Schwarz M, Knauer R, Lehle L (2005). Yeast oligosaccharyltransferase consists of two functionally distinct sub-complexes, specified by either the Ost3p or Ost6p subunit. FEBS Lett 579, 6564–6568.
Silberstein S, Collins PG, Kelleher DJ, Gilmore R (1995). The essential OST2 gene encodes the 16-kD subunit of the yeast oligosaccharyltransferase, a highly conserved protein expressed in diverse eukaryotic organisms. J Cell Biol 131, 371–383.
Soste M, Picotti P (2013). A complete mass-spectrometric map of a eukaryotic proteome. Chimia 67, 684–684.
Spear ED, Ng DTW (2005). Single, context-specific glycans can target misfolded glycoproteins for ER-associated degradation. J Cell Biol 169, 73–82.
Spirig U, Bodmer D, Wacker M, Burda P, Aebi M (2005). The 3.4-kDa Ost4 protein is required for the assembly of two distinct oligosaccharyltransferase complexes in yeast. Glycobiology 15, 1396–1406.
Spirig U, Glavas M, Bodmer D, Reiss G, Burda P, Lippuner V, te Heesen S, Aebi M (1997). The STT3 protein is a component of the yeast oligosaccharyltransferase complex. Mol Gen Genet 256, 628–637.
Springer M, Weissman JS, Kirschner MW (2010). A general lack of compensation for gene dosage in yeast. Mol Syst Biol 6, 368.
te Heesen S, Knauer R, Lehle L, Aebi M (1993). Yeast Wbp1p and Swp1p form a protein complex essential for oligosaccharyl transferase activity. EMBO J 12, 279–284.
Thibault G, Ng DTW (2012). The endoplasmic reticulum-associated degradation pathways of budding yeast. Cold Spring Harb Perspect Biol 4, a013193.
Torres EM, Dephoure N, Panneerselvam A, Tucker CM, Whittaker CA, Gygi SP, Dunham MJ, Amon A (2010). Identification of aneuploidy-tolerating mutations. Cell 143, 71–83.
Torres EM, Sokolsky T, Tucker CM, Chan LY, Boselli M, Dunham MJ, Amon A (2007). Effects of aneuploidy on cellular physiology and cell division in haploid yeast. Science 317, 916–924.
Travers KJ, Patil CK, Wodicka L, Lockhart DJ, Weissman JS, Walter P (2000). Functional and genomic analyses reveal an essential coordination between the unfolded protein response and ER-associated degradation. Cell 101, 249–258.
Vogel C, Marcotte EM (2012). Insights into the regulation of protein abundance from proteomic and transcriptomic analyses. Nat Rev Genet 13, 227–232.
Wach A, Brachat A, Pohlmann R, Philippsen P (1994). New heterologous modules for classical or PCR-based gene disruptions in Saccharomyces cerevisiae. Yeast 10, 1793–1808.
Weaver BA, Cleveland DW (2006). Does aneuploidy cause cancer? Curr Opin Cell Biol 18, 658–667.
Wisniewski JR, Zougman A, Mann M (2009). Combination of FASP and StageTip-based fractionation allows in-depth analysis of the hippocampal membrane proteome. J Proteome Res 8, 5674–5678.
Xie W, Kanehara K, Sayeed A, Ng DTW (2009). Intrinsic conformational determinants signal protein misfolding to the Hrd1/Htm1 endoplasmic reticulum-associated degradation system. Mol Biol Cell 20, 3317–3329.
Yan AX, Ahmed E, Yan Q, Lennarz WJ (2003). New findings on interactions among the yeast oligosaccharyl transferase subunits using a chemical cross-linker. J Biol Chem 278, 33078–33087.